REVIEW

EDUCATIONAL SERIES IN CONGENITAL HEART DISEASE: Tetralogy of Fallot: diagnosis to long-term follow-up

R Bedair MB BCh (Hons) MSc MD FRCP[1] and **X Iriart MD[2]**

[1]Department of Adult Congenital Cardiology, Bristol Heart Institute – University Hospitals Bristol NHS Foundation Trust, Bristol, UK
[2]Department of Pediatric and Adult Congenital Cardiology, Hôpital Cardiologique du Haut-Lévêque, CHU de Bordeaux, Pessac, France

Correspondence should be addressed to R Bedair: Radwa.Bedair@UHBristol.nhs.uk

Abstract

Tetralogy of Fallot (TOF) is the most common cyanotic congenital heart defect, affecting 3 in 10,000 live births. Surgical correction in early childhood is associated with good outcomes, but lifelong follow-up is necessary to identify the long-term sequelae that may occur. This article will cover the diagnosis of TOF in childhood, the objectives of surveillance through adulthood and the value of multi-modality imaging in identifying and guiding timely surgical and percutaneous interventions.

Key Words

► congenital heart disease
► multi-modality imaging
► pulmonary regurgitation
► tetralogy of Fallot

Introduction

Tetralogy of Fallot (TOF) is the most common cyanotic heart defect affecting 3 per 10,000 live births (1, 2, 3). The four hallmark features of the malformation (Fig. 1) are subpulmonary (and pulmonary) stenosis, ventricular septal defect (VSD), aortic override and right ventricular (RV) hypertrophy.

TOF encompasses a large spectrum of anatomical presentations, ranging from VSD with limited aortic overriding and mild pulmonary obstruction at one end of the spectrum to a critical form of VSD with pulmonary atresia (4) at the other end. It can also be associated with additional lesions such as common atrioventricular septal defect, being included in the spectrum of double-outlet RV when the aortic override is severe or present with a variant form such as TOF with absent pulmonary valve.

The Congenital Heart Surgeons' Society has recommended a nomenclature to classify TOF into three subtypes:

– TOF with varying degrees of pulmonary stenosis.
– TOF with common atrio-ventricular canal (AVSD).
– TOF with absent pulmonary valve.

Morphology

Cono-truncal anatomy

The main phenotypic feature of TOF is an antero-cephalad deviation of the muscular outlet septum. This leads to narrowing of the right ventricular outflow tract (RVOT) including infundibular stenosis in almost all cases and an abnormal pulmonary valve, which is often small and bicuspid. This is associated with various degrees of main and branch pulmonary artery hypoplasia. The evaluation of the pulmonary artery branch size is of critical importance for the surgical repair. It is usually assessed by non-invasive imaging using transthoracic echocardiography and cross-sectional imaging (see below) to establish the absolute measurements and the Nakata index (defined as the area of the right and left pulmonary arteries at the hilum in the cranio-caudal axis before the origin of the first branch divided by body surface area). A Nakata index >100 mm²/m² is associated with better survival after complete repair compared to smaller indices (5). A disconnected pulmonary artery may be present. This mainly affects the left pulmonary artery that is usually connected to the ductus arteriosus.
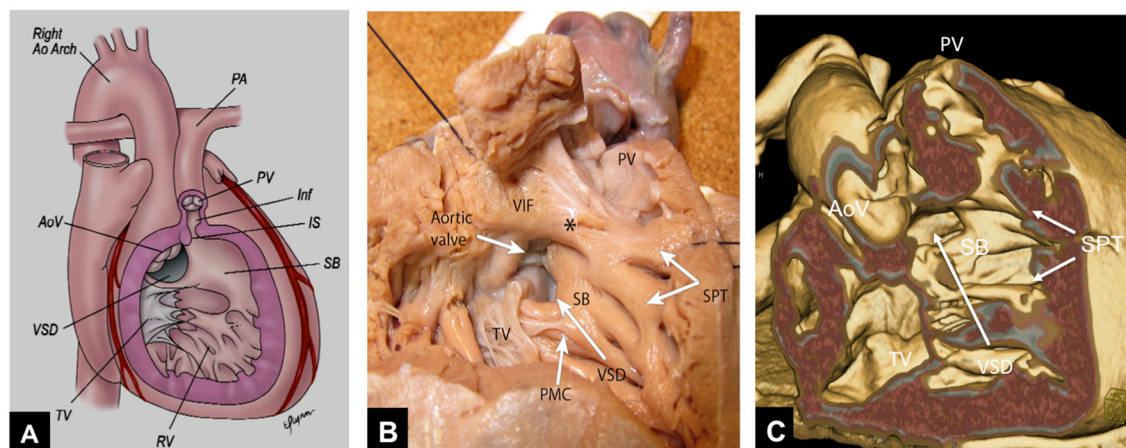
Figure 1

(A) Classical tetralogy of Fallot with obstructive infundibular, valvular and pulmonary components. (B) The photograph, taken from the apex of the morphologically right ventricle looking towards the base, and the computed tomography of the anatomic model (C), show the phenotypic features of tetralogy of Fallot: antero-superior displacement of the conal septum causing moderate stenosis of the right ventricular outflow tract, and a VSD due to the misalignment of the outlet septum. The heart has been sectioned to replicate the oblique subcostal echocardiographic cut (Fig. 5). AoV, aortic valve; PV, pulmonary valve; RV, right ventricle; SB, septal band; SPT, septo parietal trabeculations; TV, tricuspid valve; VIF, ventriculo infundibular fold; VSD, ventrciular septal defect.

A disconnected right pulmonary artery is rare, but if present, would usually arise from the ascending aorta.

Mid-cavity right ventricular obstruction, secondary to hypertrophy of the moderator band and apical trabeculations may be present, causing what is described as the 'double-chambered right ventricle' in some cases.

Ventricular septal defect

The VSD is usually in the perimembranous region (80%). Rarely, it can be juxta-arterial (or doubly committed), with its cephalad margin formed by the aortic and pulmonary valves. The VSD is usually single and non-restrictive. In rare cases, the VSD can be restrictive because of overlying accessory tricuspid valve tissue.

Coronary artery anatomy

A clockwise rotation of the aortic root is usually encountered in TOF leading to a rotated origin of the coronary arteries. Anomalies of the origin of the coronary arteries are reported in approximately 5% of cases, the most common being a left anterior descending artery arising from the right coronary artery and crossing anterior to the RVOT (6) (Fig. 2). This abnormal pattern is of critical importance for surgical repair as it may require the use of a right ventricular-to-pulmonary arterial (RV–PA) conduit. Others anomalies include the presence

of a dual LAD in 1.8%, a single RCA in 0.3%, and a coronary-to-pulmonary fistula in 0.2% (7).

Aortic arch anomalies

A right aortic arch has been reported in 25% of TOF patients and may be associated with an aberrant origin of the left subclavian artery. Rarely, a double aortic arch or a cervical arch may be present. This is frequently encountered in patients with 22q11 deletion syndrome.

Variant forms and associated lesions

TOF with absent pulmonary valve syndrome

TOF with absent pulmonary valve has been reported in 3–6% of all TOF (8). This anatomic form is characterized by typical anterior malalignment of the outlet septum associated with the usual overriding of the aorta. The particularity of this variant is an abnormal pulmonary valve characterized by a hypoplastic annulus and absent or rudimentary pulmonary valve leaflets leading to both stenosis and severe regurgitation. This physiology leads to a progressive dilatation of the pulmonary artery branches that can be associated with various degree of tracheomalacia and bronchomalacia with possible airway compression (Figs 3 and 4). The prognosis of TOF with absent pulmonary valve is much more severe than the usual form of TOF.
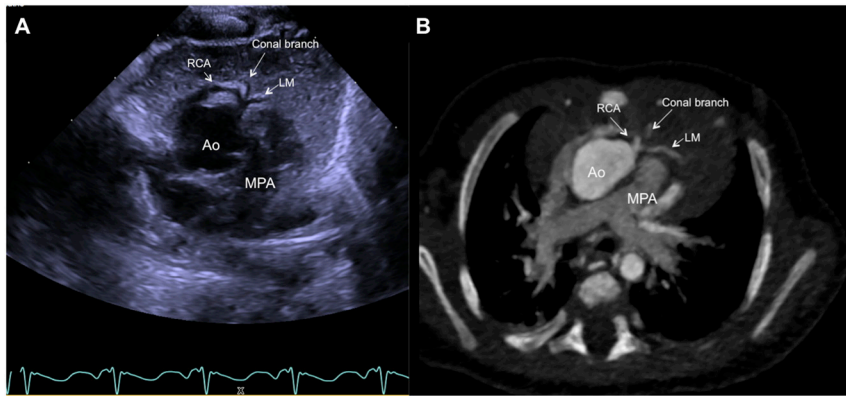
Figure 2
Coronary artery arrangement in patients with TOF. Parasternal short-axis echo image (A) and CT angiogram (B) showing an aberrant left main (LM) coronary artery arising from the right coronary artery (RCA) and crossing the RVOT, as well as a large conal branch in a patient with TOF. Ao, aorta; MPA, main pulmonary artery.

TOF with atrioventricular septal defect

Atrioventricular septal defect in association with TOF has been reported in 1.7% (8) of all TOF and is typically associated with chromosomal abnormalities, especially Trisomy 21 (Fig. 5).

Imaging of preoperative TOF

Echocardiography

Fetal echocardiography

Fetal echocardiography performed from 13 to 14 weeks of gestation can usually make the diagnosis of TOF, showing a large VSD with overriding of the aorta and antero-cephalad deviation of the outlet septum and small pulmonary arteries. The evolution of the RVOT obstruction can be monitored by serial echocardiograms throughout gestation (9). In patients with TOF with absent pulmonary valve, severe forms may lead to hydrops fetalis or fetal death.

Transthoracic echocardiography

Echocardiography is the main modality for diagnosis and follow-up of TOF. Once TOF is suspected in the neonate, a detailed echocardiographic evaluation is undertaken, including 2D, color and spectral Doppler imaging.

A comprehensive and detailed description using the segmental approach is performed in a systematic manner by the echocardiographer (6).

The goals of the initial evaluation can be summarized as follows:

– Presence or absence of thymus.
– Visceral and atrial situs.
– Pulmonary and systemic venous connection and any type of atrial septal defects.
– AV valves morphology and function (look for AVSD anatomy).
– VSD morphology and shunting direction.
– LV and RV size, morphology and function.
– Cono-truncal anatomy and degree of stenosis of the RV outflow tract.
– Pulmonary annulus size and valve morphology.
– Main pulmonary and pulmonary artery branch size. Rule out abnormality of origin or course of a pulmonary artery (sling or disconnected LPA following PDA closure).
– Aortic arch sidedness and branching pattern.
– PDA origin and patency or aorto-pulmonary collaterals.
– Coronary artery anatomy.

Subcostal long axis view

A sweep of the transducer from this view can easily assess the systemic and venous connections to the heart,
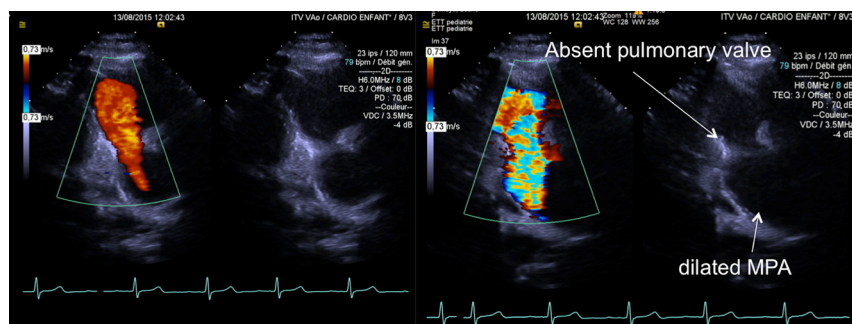

Figure 3
TOF with absent pulmonary valve and hypoplastic annulus: free pulmonary regurgitation (left panel); color Doppler flow acceleration in systole (right panel) and dilated MPA. MPA, main pulmonary artery.
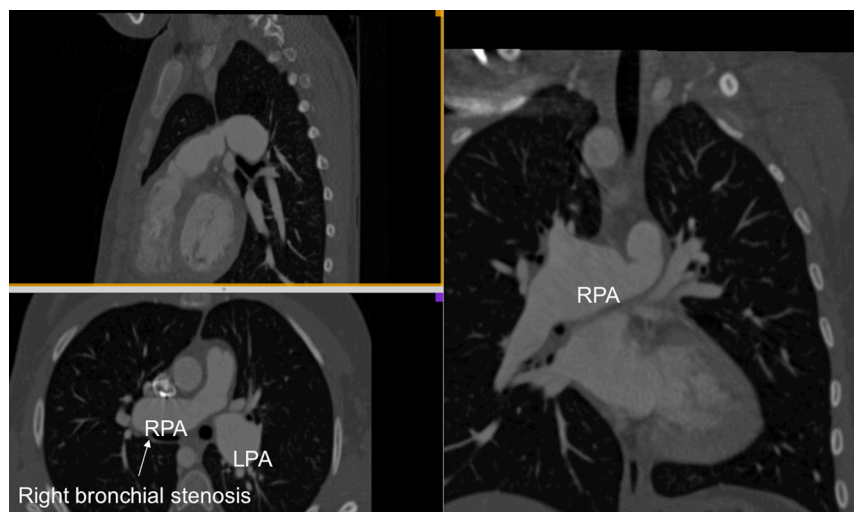
Figure 4
Repaired TOF with absent pulmonary valve. Aneurysmal dilatation of the branch pulmonary arteries with the RPA causing right bronchial narrowing. LPA, left pulmonary artery; RPA, right pulmonary artery.

the atrial septum and the normal atrioventricular and ventriculo-arterial connections. The VSD, with the overriding aorta and the RVOT obstruction caused by the antero-cephalad deviation of the outlet septum can also be identified. The right pulmonary artery can usually be assessed from this view, the left pulmonary artery being more difficult to see given its orientation.

Subcostal short-axis view

The subcostal short-axis view is classically used for viewing the antero-cephalad deviation of the outlet septum and the level of the RVOT obstruction. This view also preferentially shows the interatrial septum and the potential presence of ASD and the type of VSD. LV and RV function are also easily identifiable. The tricuspid and the mitral valves can be viewed 'en face' and particular attention should be given to not miss a cleft or an associated AVSD (Fig. 6).

Apical views

The apical four- and five-chamber views classically demonstrate the mitral and tricuspid valve morphology, the biventricular function and the VSD. The entire septum should be interrogated for additional muscular VSDs.

Parasternal long axis view

The parasternal long axis view usually demonstrates the type of VSD and the degree of overriding of the aorta. In TOF the aorta overrides the VSD by less than 50% of the aortic diameter, while in DORV the override is more than 50%. The presence of aorto-mitral continuity also distinguishes TOF from a DORV. An anterior sweep of the transducer allows the evaluation of the RVOT and the pulmonary valve to assess the potential

level of stenosis and the size of the pulmonary valve annulus (Fig. 7).

Parasternal short-axis view

This view provides additional information about the VSD margins and the RVOT anatomy. The pulmonary valve morphology and its size can be assessed as well as the main PA diameter. The coronary artery anatomy is preferentially visualized from this view. An optimization of the color Doppler settings (lowering the Nyquist limit) is helpful to enhance the flow velocity in the coronary arteries. An abnormal origin of the LAD artery arising from the right coronary artery and crossing anterior to the right ventricular outflow tract, or presence of dual LAD
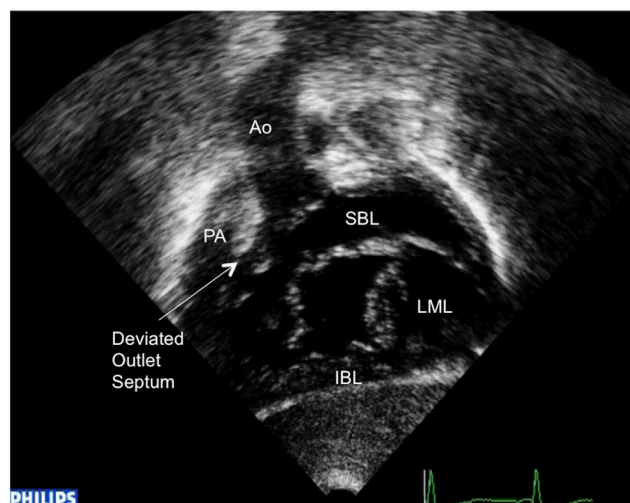

Figure 5
TOF-AVSD. Subcostal short-axis images at the level of the AV valve valve showing an en face view of the common AV valve (SBL, superior bridging leaflet, IBL, inferior bridging leaflet, LML, left mural leaflet are seen) and the deviation of the outlet septum.
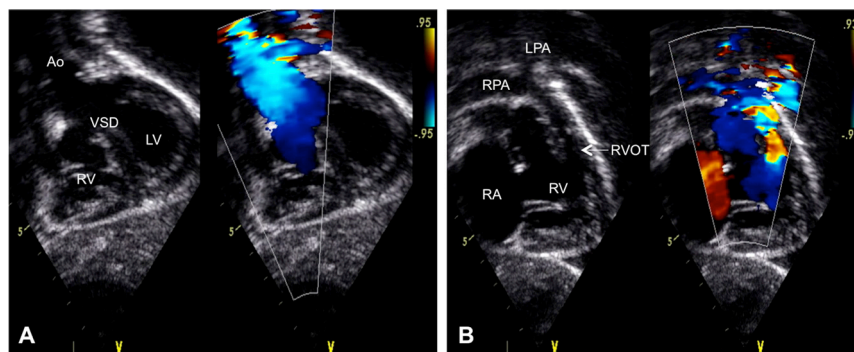
Figure 6
Subcostal view. Subcostal short-axis view showing the overriding aorta and non-restrictive VSD with laminar flow on color flow mapping (A). Modified anterior oblique subcostal view shows the length of RVOT, pulmonary valve and branch pulmonary arteries in detail. Flow turbulence on color flow mapping confirms infundibular obstruction. Ao, aorta; LPA, left pulmonary artery; LV, let ventricle; RA, right atrium; RV, right ventricle; RVOT, right ventricular outflow tract; VSD, ventricular septal defect.

coronary arteries or a major infundibular branch should be sought (Fig. 2).

Suprasternal view

This view demonstrates the aortic arch sidedness and the aortic branching pattern. Establishing aortic side and branching pattern is important in patients with severe TOF, especially in those referred for palliative shunt such as a modified Blalock–Taussig shunt, as the shunt is performed on the opposite side of the arch sidedness (i.e. right shunt in a left sided arch).

Any other vascular ring or aortic arch malformation (cervical arch) can be assessed from this view as well as retroaortic innominate vein or left superior vena cava draining into the coronary sinus.
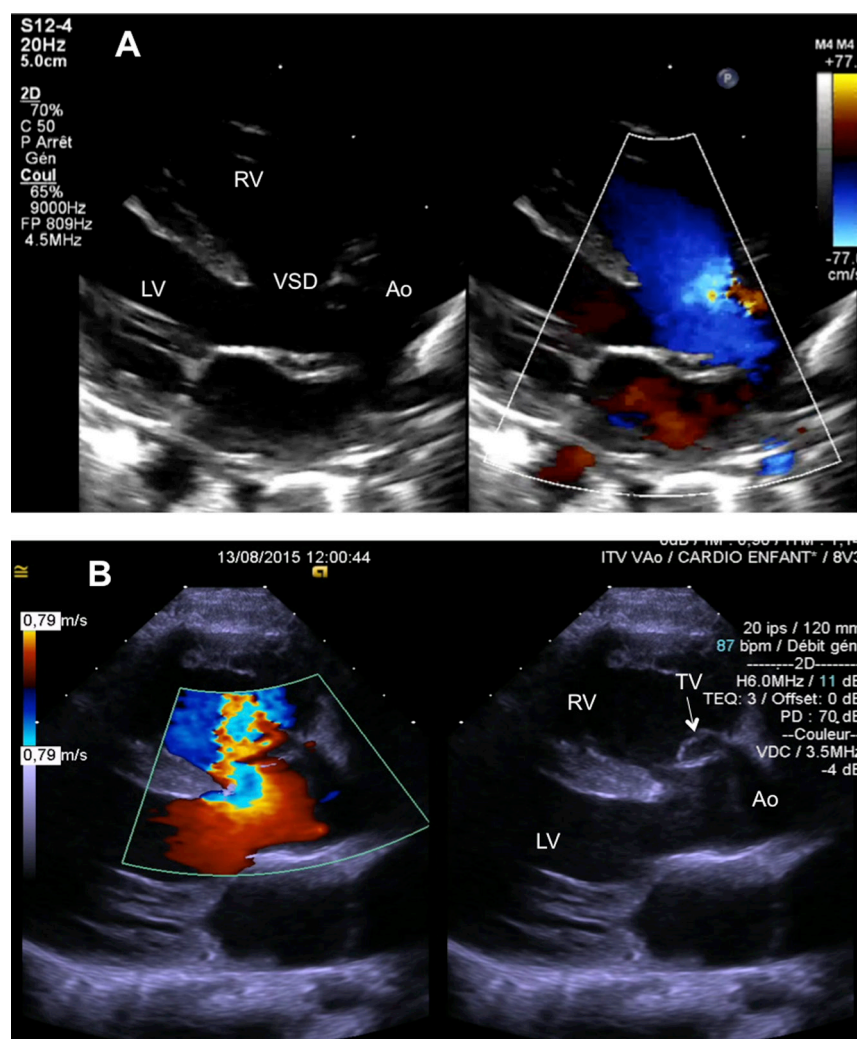

Figure 7
Parasternal long axis view. Parasternal long axis view showing a non-restrictive VSD (A) with right to left shunting and a restrictive VSD (B) with tricuspid leaflet tissue seen in the 2D imaging within the VSD. Ao, aorta; LV, left ventricle; RV, right ventricle; TV, tricuspid valve; VSD, ventricular septal defect.

Cardiovascular magnetic resonance imaging

In the preoperative TOF patient, if echocardiography has not permitted an exhaustive evaluation of the intracardiac and extra-cardiac structures, cardiovascular magnetic resonance (CMR) represents an alternative to provide the missing information for diagnosis and surgical planning. Different sequences are recommended for imaging different conditions (10), but CMR protocols usually include:

– Anatomical assessment of the heart and the vessels using spin echo imaging.
– Dynamic (cine) assessment of the cardiac chambers and of left and right ventricular outflow tracts in two orthogonal planes. Additional acquisitions can be performed for pulmonary artery branches or aortic assessment.
– MR angiography of the pulmonary artery branches and the aorta.

The main drawbacks of CMR are the lack of availability and technical aspects that require breath-holding or acquisition over multiple cardiac cycles for cine imaging and lower spatial and temporal in contrast to other imaging modalities. Cardiac MRI studies often require general anesthesia in infants and young children (10). CMR may be useful in selected young children with lesions such as aortic arch anomalies and disconnected branch pulmonary arteries to delineate full extra-cardiac anatomy pre surgery.

Computed tomography

Recent advances in acquisition techniques including radiation exposure reduction make CT a real alternative to CMR in addition to the first-line echocardiographic evaluation. CT has an excellent spatial resolution (<0.5 mm) and the acquisition time currently lasts only a few seconds. Its main drawback is the use of ionizing radiation, which raises concerns especially in the pediatric population. High lifetime cumulative doses from X-rays, cardiac CT, diagnostic and interventional cardiac catheterization in these patients should be borne in mind when considering the use of serial cardiac CT (11). In recent years, a number of dose-reduction techniques have been instituted, with preservation of image quality. With prospective systolic gating, delivered doses in a pediatric population can range between 0.6 mSv and 1.1 mSv (12) (compared to approximately 0.1 mSv for a chest X-ray) to image the coronary arteries and define thoracic vascular anatomy. This can be helpful for surgical planning in the most severe forms of TOF including TOF with pulmonary

atresia or, at the other end of the spectrum, TOF with absent pulmonary valve. Cardiac CT may offer an alternative for anatomic evaluation, meaning that cardiac catheterization can be reserved for cases requiring catheter intervention.

Angiography

Angiography had been, for decades, the imaging gold standard for the preoperative assessment of TOF. Advances in cross-sectional imaging currently allow non-invasive definition of the anatomic details of intracardiac and extra-cardiac structures, including pulmonary branch anatomy or coronary artery pattern. X-ray angiography remains an alternative imaging modality when it supports percutaneous interventions.

Surgical repair of TOF

The first palliation for TOF was performed in 1945 and is named after the surgeon (Blalock) and cardiologist (Taussig) who first described it. This was a systemic-to-pulmonary artery shunt and involved the anastomosis of the right subclavian end-side to the right pulmonary artery: The Blalock–Taussig (BT) shunt (13). Presently, only a minority of patients require an initial palliative procedure to increase pulmonary blood flow or to allow for growth of the main and branched pulmonary arteries. Current palliation, if necessary, is in the form of systemic-pulmonary artery shunts and more recently by stenting of the RVOT (14).

The first complete repair of TOF was performed by Lillehei in 1954 (15). Corrective surgery involves patch closure of the VSD, leaving the aorta committed to the left ventricle and provides relief to the right ventricular outflow tract, pulmonary valve or branch pulmonary artery obstruction. The relief of the RVOTO is usually at the expense of leaving behind a degree of pulmonary regurgitation, particularly if a trans-annular patch is used. Patients with anomalous coronary arteries and/or absent pulmonary valve will require RV–PA conduits at the time of the first corrective surgical procedure, with the need for subsequent revisions.

Long-term follow-up after surgical repair of TOF

Repaired TOF is associated with good long-term outcomes with a long-term survival of 90% (16). There are though, a recognized number of long-term hemodynamic,

electrical and anatomical sequelae. All patients with repaired TOF need lifelong clinical reviews and serial, often multi-modality, cross-sectional imaging to allow for timely management of the long-term sequelae, discussed in the following sections.

Pulmonary regurgitation

Pulmonary regurgitation is the most frequently encountered hemodynamic lesion following surgical repair of TOF. It can range from mild to severe and is described as free pulmonary regurgitation when there is no effective valve function, seen with the placement of a trans-annular patch. Pulmonary regurgitation leads to progressive right ventricular dilatation and possible late dysfunction. This is usually a well-tolerated lesion and most patients remain symptom free for decades, but the majority with a severe lesion will require pulmonary valve replacement, often in the third decade of life. Pulmonary valve replacement is, at present, the most frequently performed procedure in adult patients with congenital heart disease. Table 1 describes the objectives of imaging and the relative value of the different imaging modalities in evaluating a patient with pulmonary regurgitation (Fig. 8).

Residual right ventricular outflow tract obstruction, pulmonary valve and branch pulmonary artery stenosis

Residual or progressive obstruction to the blood flow from the right ventricle to the branch pulmonary arteries can be encountered and can be related to the original morphology (e.g. the original size of the branch pulmonary arteries). It can be seen at multiple levels, including residual infundibular obstruction, small pulmonary annulus, degeneration and progressive obstruction in replaced pulmonary valves and conduits and branch pulmonary artery stenosis. The objectives from imaging are the identification of the severity and level(s) of obstruction and the effects on the right ventricle and the relative merits of the different imaging modalities in this setting are described in Table 2 (Fig. 9).

Right ventricular enlargement and dysfunction

Pulmonary regurgitation represents a chronic volume overload on the right ventricle that leads to progressive right ventricular dilatation. Residual obstruction represents a chronic pressure overload and leads to right ventricular hypertrophy. Both lesions, if severe and un-addressed in a timely manner, can cause right ventricular systolic dysfunction. The diastolic function of the right ventricle is also often affected by the original lesion, cardiopulmonary bypass and post-repair hemodynamic lesions. A restrictive RV physiology represents the physiological manifestations detected with Doppler of a non-compliant right ventricle. It is often seen in the presence of RV obstruction, but may co-exist with pulmonary regurgitation. This can limit the degree of pulmonary regurgitation due to early equalization between the PA and RV pressures and may limit RV enlargement (Figs 10 and 11).

Tricuspid regurgitation

Tricuspid regurgitation can be seen with progressive right ventricular enlargement that leads to annular dilatation, but leaflet abnormalities can also be encountered and may be related to the tethering in the region of the VSD patch. A careful evaluation of the severity and mechanism of tricuspid regurgitation is needed. Consideration should be given to the need for tricuspid valve repair or replacement at the time of pulmonary valve surgery.

Aortic root dilatation and aortic regurgitation

Although aortic root enlargement is frequently seen and a root measuring ≥40 mm affects a third of patients (17), progressive dilatation or dilatation that requires primary aortic root replacement is rare. Annular dilatation can

Table 1 Objectives and relative value of multi-modality imaging in the assessment of pulmonary regurgitation in repaired ToF.

	Echocardiography	CMR	Cardiac CT	Cardiac catheterization and angiography
Presence and severity of pulmonary regurgitation	✓✓	✓✓✓		✓
Quantify RV dilatation and function	✓✓	✓✓✓	✓*	✓
Assess associated valve lesions	✓✓✓	✓✓		✓
Planning percutaneous interventions	✓	✓✓	✓✓✓	✓✓✓

*This is usually reserved for patients with limited echo windows and a contra-indication to cardiac MRI.
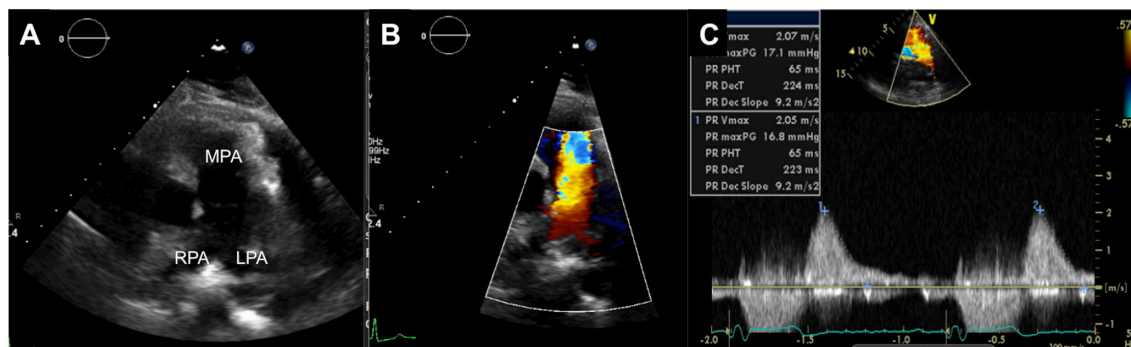CMR, cardiac magnetic resonance; CT, computed tomography.

Figure 8

Severe pulmonary regurgitation in a patient with repaired TOF. Parasternal short-axis window showing the main (MPA) and branch pulmonary arteries on 2D imaging (A) with pulmonary regurgitation on color flow mapping occupying the width of the MPA and originating from the two branches (B), with a short pressure half time (65 ms) on spectral Doppler imaging (C). LPA, left pulmonary artery; MPA, main pulmonary artery; RPA, right pulmonary artery.

lead to aortic regurgitation, and this can rarely become a progressive lesion that requires surgical intervention.

Left ventricular dysfunction

Left ventricular systolic and diastolic dysfunction can be seen in patients with repaired TOF and is well described in older patients who underwent late repair. Causes for left ventricular dysfunction include ventriculo-ventricular interaction, cyanosis with late repair, ventriculotomy performed in earlier surgery, concomitant coronary artery disease in an aging patient population and secondary to sustained, uncontrolled atrial arrhythmia which are frequently seen. Left ventricular function is an important predictor of arrhythmia and survival.

Arrhythmia and aborted sudden death

Atrial arrhythmias are common in patients with repaired TOF and are secondary to atrial scar and atrial stretch with elevated pressures. Ventricular arrhythmia including ventricular tachycardia, ventricular fibrillation and sudden death are well described (18). Imaging can help identify correctable hemodynamic lesions, evaluate biventricular function and image areas of scar.

This can help guide therapeutic interventions with fusion of CMR images with electro-anatomical maps (Fig. 12). With aborted sudden death, implantable defibrillators (ICD) are used which impact the future choice of imaging modality. CMR was conventionally contraindicated in the presence of implantable cardiac devices, but MRI conditional devices are now widely used in patients with repaired congenital heart disease, although the artifact generated may lead to non-diagnostic image quality. Transvenous ICD leads can affect tricuspid valve function. The objectives and different modalities of imaging with respect to the assessment of the risk of occurrence or recurrence of cardiac arrhythmia are shown in Table 3.

Multi-modality imaging after TOF repair

Echocardiography

Serial echocardiograms are recommended and should be performed at routine intervals.

Subcostal view

This may provide limited views in adult patients. Visualizing the IVC as well as assessing hepatic vein flow

Table 2 Objectives and relative value of multi-modality imaging in the assessment of right ventricular outflow tract, pulmonary valve, main and branch pulmonary artery obstruction in repaired ToF.

	Echocardiography	CMR	Cardiac CT	Cardiac catheterization and angiography
Severity of RVOTO	✓✓✓	✓✓✓	✓	✓✓
Level of RVOTO	✓✓	✓✓	✓✓✓	✓✓
Quantify RV function	✓✓	✓✓✓	✓	✓
Assess associated valve lesions	✓✓✓	✓✓		✓
Planning percutaneous interventions	✓	✓✓	✓✓✓	✓✓✓

CMR, cardiac magnetic resonance; CT, computed tomography; RV, right ventricle; RVOTO, right ventricular outflow tract obstruction.
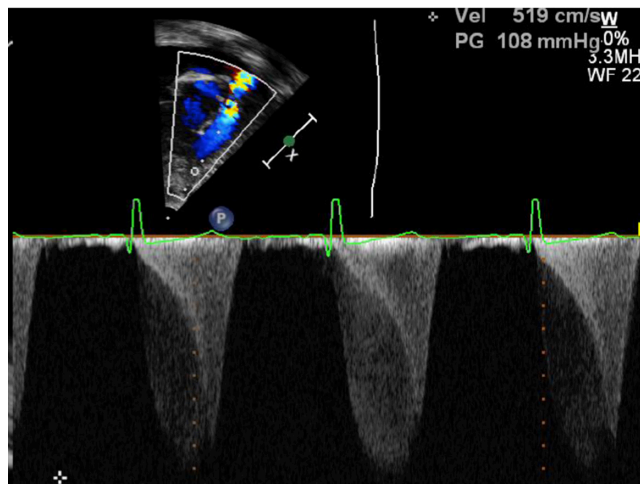
Figure 9
Multi-level RV outflow tract assessment by CW Doppler. Spectral Doppler showing severe obstruction (peak velocity 5.2 m/s, peak gradient 108 mmHg) across RV infundibulum (Dagger shaped envelope) and pulmonary valve (symmetrical envelope). CW, continuous wave; RV, right ventricle.

gives an indication of right atrial pressure, tricuspid valve function and diastolic right ventricular function.

Parasternal long axis view

The RV free wall is visualized and RV hypertrophy is readily identifiable. A visual assessment of RV free wall function and RV size can be made. The VSD patch can be visualized and assessed for residual VSDs. The aortic root and ascending aorta can be assessed. Moving up one intercostal space will bring more of the ascending aorta into view. Inferior angulation of the probe brings the tricuspid valve into view and superior angulation

brings the pulmonary valve and main pulmonary artery into view.

Parasternal short-axis view

This is the best view for the analysis of the pulmonary valve, but modified views may be needed particularly for conduits that are in very anterior positions. 2D imaging evaluates the size of the RV, RV outflow tract (RVOT1, RVOT2), size of the pulmonary valve annulus, mobility of the pulmonary valve leaflets and size of the main pulmonary artery and its branches. The RV dilatation may be more evident in this view given the anterior dilatation that occurs in repaired TOF, especially with the use of a trans-annular patch during surgical repair. Detailed evaluation of the branch pulmonary arteries is often limited in adult patients. Color flow mapping readily identifies pulmonary regurgitation and RVOT obstruction if present. Pulsed-wave and continuous wave Doppler interrogation of the RV outflow tract, pulmonary valve and MPA can grade severity of both pulmonary regurgitation and stenosis. In the presence of multi-level RVOTO, an estimate of RV pressure is best derived from the TV regurgitant jet if present. Severe pulmonary regurgitation is identified using the criteria in Table 4. Restrictive right ventricular physiology is diagnosed when there is pre-systolic forward flow through the pulmonary valve seen on the RVOT/PV spectral Doppler trace with atrial contraction, described as an 'a wave'.

Apical view

This is the view that allows the most comprehensive assessment of chamber sizes and both right and left ventricular function. Measurements should be made in line
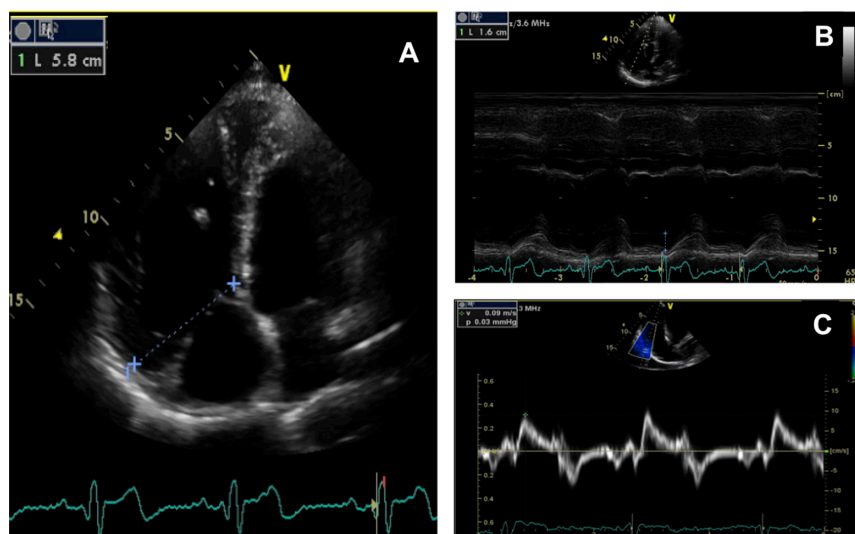

Figure 10
Dilated right ventricle in a patient with repaired TOF and severe pulmonary regurgitation. Apical four chamber view in a patient with repaired TOF and severe pulmonary regurgitation before pulmonary valve replacement surgery, showing dilated right ventricle: RVD1 58 mm and right atrium, (A) and mildly reduced indices of basal longitudinal function, TAPSE 16 mm (B) and tricuspid annular TDI showing an S′ of 9 cm/s (C). RVD, right ventricle dimension; TAPSE, tricuspid annular systolic plane excursion; TDI, tissue Doppler imaging.
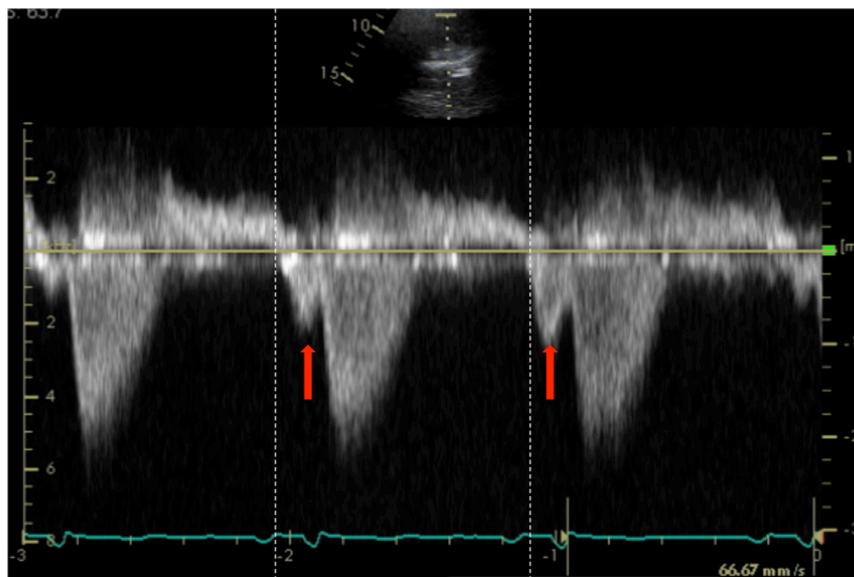
Figure 11
'Restrictive RV' physiology on spectral Doppler. Spectral Doppler across the pulmonary valve in a patient with previous TOF repair showing the characteristic 'A' wave (red arrow) in a patient with a restrictive RV. This pre-systolic forward flow in the pulmonary artery is caused by the pressure generated by right atrial contraction (dashed line indicating end of atrial contraction) transmitted through the right ventricle to the RVOT and causing pre-systolic opening of the pulmonary valve. RV, right ventricle; RVOT, right ventricular outflow tract.

with published recommendations and guidelines (19), but this should be coupled with an appreciation of the lack of data to support the reproducibility of the measurements and their correlation with CMR quantification, which remains the gold standard. 2D end-diastolic measures of RV size include basal (RVD1) and mid-cavity (RVD2) dimensions as well as RV length, and end-systolic right atrial area. RV hypertrophy and abnormalities of septal motion can be used as indirect indicators of RV pressure, but the almost uniform presence of right bundle branch block in these patients makes the reliance on septal motion to evaluate RV pressure of limited clinical utility.

An evaluation of right ventricular or pulmonary artery pressure can be made from this view in the presence of tricuspid regurgitation. Doppler alignment with the TR jet is often possible and couple with an estimate of RA pressure (usually using the IVC size and reactivity, the modified Bernoulli equation can be used).

Global and regional indices of RV systolic function should be measured serially and include the following quantitative measures (cut-off normal values, derived from non-congenital heart disease-based normative data in adults are detailed in Table 5 (19)):
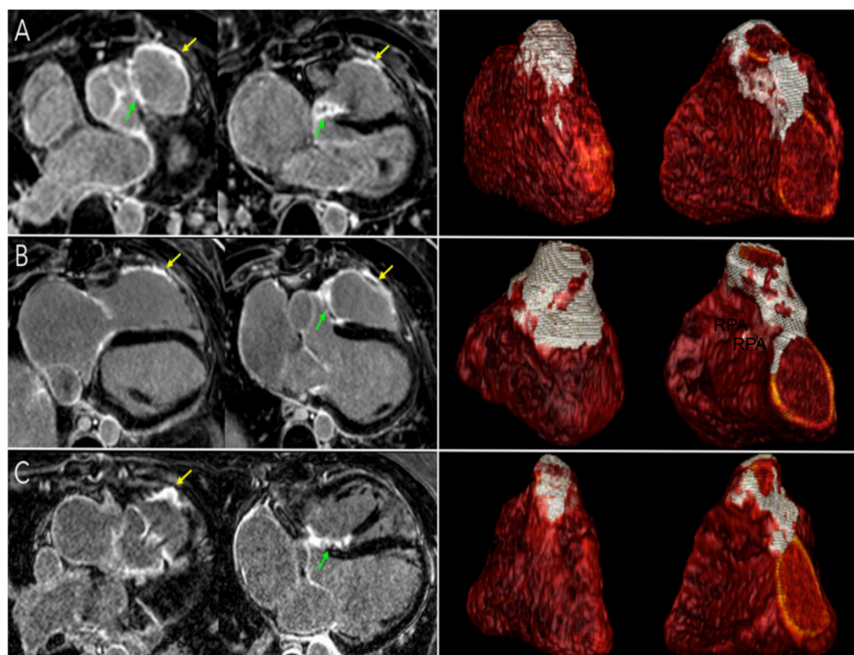

Figure 12
Examples of scar distributions on high-resolution LGE images in patients with repaired TOF. LGE data from three patients are shown (A, B and C). Trans-axial LGE images are shown in the left column, yellow and green arrows indicating RVOT and septal scars, respectively. In the right column, the corresponding scar distributions are displayed in RVOT and septal views (left and right images, respectively). LGE, late gadolinium enhancement; RVOT, right ventricular outflow tract.

Table 3 Objectives and relative value of multi-modality imaging in the assessment of arrhythmia risk in repaired ToF.

	Echocardiography	CMR	Cardiac CT	Cardiac catheterization, angiography and electro-anatomical mapping
Identification of (reversible) hemodynamic lesions	✓✓✓	✓✓✓		✓✓
Quantification of chamber size and ventricular function	✓✓✓	✓✓✓	✓	✓
Imaging of myocardial scar		✓✓✓*		✓✓*

*Fusion imaging with electro-anatomical mapping.

a. TAPSE – tricuspid annular systolic planar excursion: M-mode assessment of the degree of excursion of the tricupisd annulus is a measure of basal RV longitudinal function. In patients with TOF it may not correlate with measures of global and regional function in other areas (20).

b. Tissue Doppler imaging of the tricuspid annulus: The velocity of the S wave on the TDI of the tricuspid annulus is similar to TAPSE in that it assesses the basal RV longitudinal function. This correlates with RVEF on CMR if the outflow tract function is preserved but less so in the presence of RVOT dyskinesia (21).

c. RV fractional area change: Calculation of the RV FAC involves tracing around the RV endocardial border in diastole and systole, excluding trabeculations, moderator band and papillary muscles and calculating the relative change. It requires good endocardial definition and the presence of prominent RV trabeculations may make finding the endocardial border more challenging. Although RV FAC correlates with RVEF on CMR, this is not validated in patients with TOF with low correlations with CMR measures of RV function (22).

d. RV global longitudinal and regional strain: This is an angle-independent measure of RV function and is of established prognostic value in non-congenital patients, but data specific to patient with repaired TOF is still sparse (23) (Fig. 13).

e. 3D RVEF: 3D echo has been validated against CMR and provides the best echocardiographic index of overall RV systolic function, but tends to under-estimate RV volumes when compared to CMR, on which a lot of the decision making for pulmonary valve intervention is based (Fig. 14).

All these indices (except for 3D RVEF) have inherent limitations given the complex geometry of the right ventricle in patients with repaired TOF. TAPSE – TDI correlating least and 3D RVEF and GLS correlating best with CMR-derived RVEF. There is also a lack of normal values for patients with repaired TOF, and variable results of studies that assess the correlation with CMR-derived measures of RV function, which is the gold standard (24, 25). Normal and abnormal values are described in the chamber quantification guidelines and can be used but a serial change is more meaningful for the clinical care of the individual patient.

Cardiovascular magnetic resonance (CMR)

CMR is the gold standard for the evaluation of both the severity of pulmonary regurgitation and the size and function of the right ventricle (Figs 15 and 16). The branch pulmonary arteries are often not well imaged on echocardiography in adults and must be evaluated with CMR scan in all patients, but in particular those with previous systemic-pulmonary artery shunts, previous branch pulmonary artery reconstruction or intervention,

Table 4 Criteria for moderate-severe pulmonary regurgitation.

Parameter	Abnormality threshold
Pulmonary regurgitation PHT	<100 ms
Jet:Annulus width ratio	0.5
Diastolic flow reversal from the branch pulmonary arteries	From branch PAs
Termination of flow in mid-late diastole	No flow time >80 ms.

PA, pulmonary artery; PHT, pressure half time.

Table 5 Normal and abnormal valves for measures of RV function in adult patients (ASE/ESC recommendations) (13).

Parameter	Abnormality threshold
TAPSE (mm)	<17
RV FAC (%)	<35
RV free wall 2D strain (%)	≥ -20
RV 3D EF (%)	<45
Pulsed Doppler S wave (cm/s)	<9.5

EF, ejection fraction; FAC, fractional area change; RV, right ventricle; TAPSE, tricuspid annular plane systolic excursion.
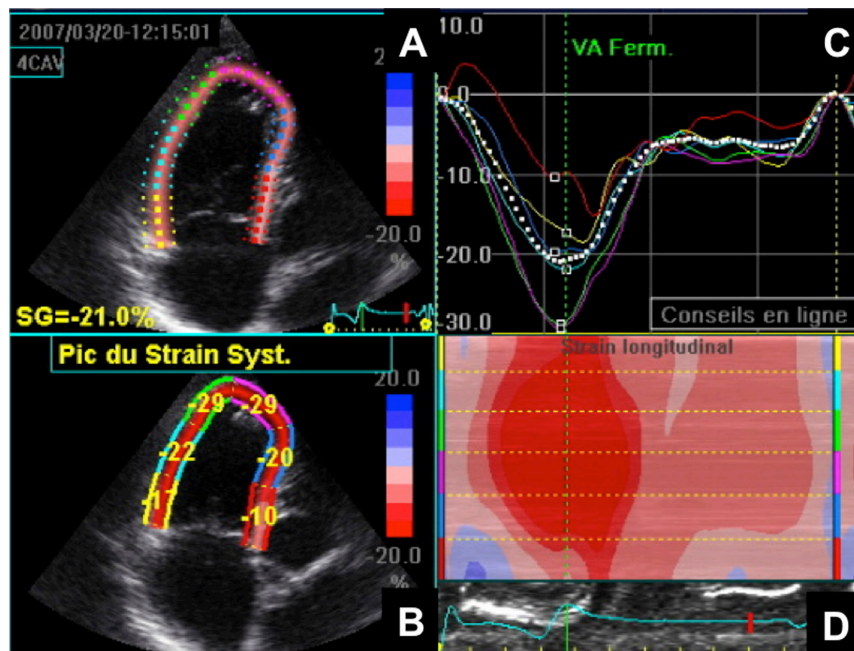
Figure 13
Right ventricular strain assessment. (A) Apical 4-chamber view with semi-automatic detection of the regions of interest. This method requires the user to outline the internal border of the myocardium. The 2D strain algorithm automatically evaluates the tracking quality at each myocardial location over time, and provides the tracking quality of each segment as either 'acceptable' (V) or 'non-acceptable' (X) in a table just below the image. (B) RV regional longitudinal peak systolic strain. (C) Myocardial longitudinal strain curves determined by speckle tracking imaging. (D) Map of the regional longitudinal strain.

with split pulmonary artery flow assessments aiding clinic decision making for branch pulmonary artery interventions. Scar imaging with gadolinium is part of routine clinical practice, and research is underway to evaluate scar-directed ablation procedures (Fig. 12). In the absence of favorable echocardiographic windows, CMR provides a comprehensive evaluation of biventricular size and function, valve function, morphology of the RVOT and branch PAs and the aortic root dimensions. MRI conditional cardiac devices, stent material and struts of bio-prosthetic and mechanical valves lead to artifact and limitations in imaging.

The indications for and timing of pulmonary valve replacement in patients with a dysfunctional pulmonary valve, especially those with pulmonary regurgitation is one of the most debated issues among congenital heart disease specialists. If patients present with cardiovascular symptoms,

not otherwise explained, and moderate-to-severe pulmonary regurgitation, pulmonary valve replacement should be considered in line with published guidelines (26, 27).

In the absence of symptoms, the timing of pulmonary valve replacement is often determined using CMR-derived indices of RV size and function after confirmation of moderate-to-severe pulmonary regurgitation (regurgitant fraction ≥25% by CMR). The CMR indices to consider include (28, 29, 30):

1. RV end-diastolic volume index >160 mL/m².
2. RV/LV end-diastolic volume ratio >2.
3. RV end-systolic volume index >80 mL/m².
4. RV ejection fraction <47%.
5. Large RVOT aneurysm.

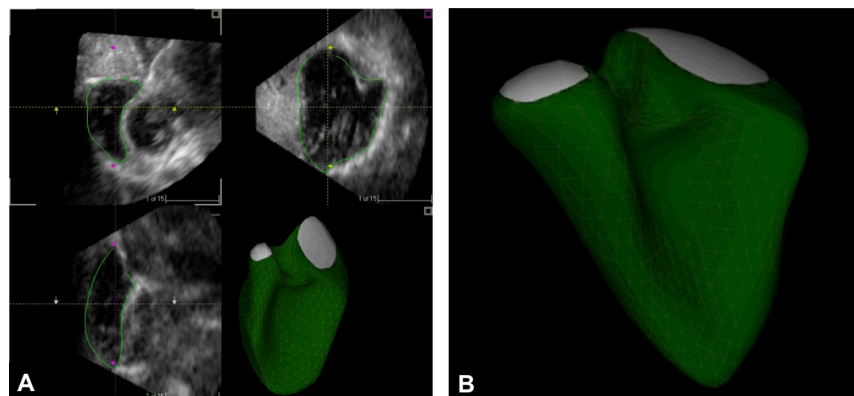Multiple CMR-based studies have tried to address the question of optimal timing for pulmonary valve

Figure 14
3D RV assessment. (A) Display from the four-dimensional RV function analysis program showing the final stage of contour detection, in which manual correction of the contours can be applied in any cross-section or phase of the cardiac cycle. (B) View of the four-dimensional RV function mesh showing RV geometry and volume. RV, right ventricle.
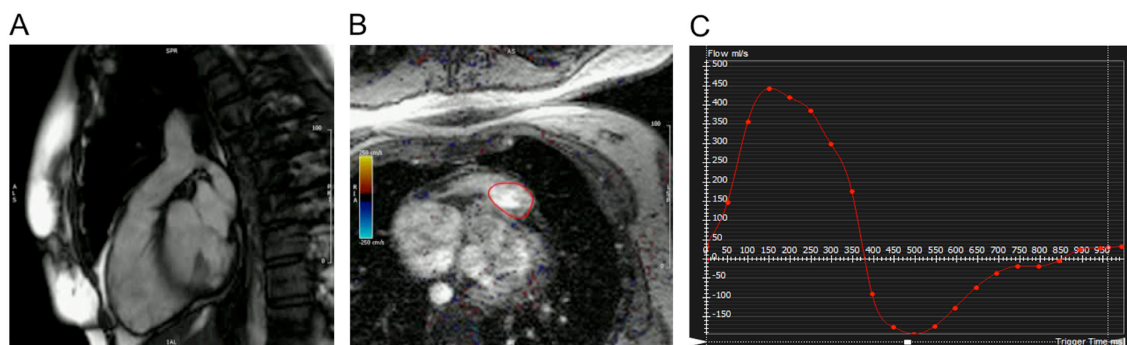
Figure 15
Use of cardiac MRI to assess severity of pulmonary regurgitation using phase-contrast imaging. (A) Sagittal view of the right ventricular outflow tract. Line (red) indicating the plane of imaging for flow in the expected position of the pulmonary valve. (B) Circle indicating assessment of flow in region of interest. (C) Flow curves from phase-contrast imaging. Pulmonary regurgitation indicated flow below the baseline (arrow). Image courtesy of Dr Michael Yeong.

replacement (30, 31), and the benefits of pulmonary valve replacement have been shown in a large meta-analysis of 48 studies, showing improvements in right ventricular size and function, improvements in left ventricular function, improvements in symptoms and positive electrical remodeling in the form of shortened QRS duration (32). Less definite is the beneficial effect of pulmonary valve replacement in terms of improving survival and decreasing sustained ventricular arrhythmia. An international registry study considering the effects of pulmonary valve replacement on clinical outcomes showed no difference in death and sustained ventricular arrhythmia following pulmonary valve replacement at 5 years of follow-up. Furthermore, this study showed more adverse events in patients who underwent 'early'

Figure 16
Cine SSFP short-axis ventricular stack for ventricular volumetric data. Dilated right ventricle indicated by arrow (white). Image courtesy of Dr Michael Yeong.

pulmonary valve replacement outside the consensus indications (33).

Cardiac CT

Cardiac gated CT has high spatial resolution and is useful in detailing anatomy, which aids planning of interventional procedures. CT is increasingly used in patients being evaluated for percutaneous pulmonary valve implantation to assess the size of the conduits and proximity to coronary arteries. Patients older than 40 years need coronary artery disease excluded prior to pulmonary valve replacement surgery and this can be achieved with CT. Fusion imaging with superimposition of cardiac CT scans on fluoroscopy at the time of cardiac catheter intervention can reduce radiation and contrast doses (34).

Cardiac catheterization and angiography

Cardiac catheterization and angiography as the primary diagnostic modality for patients with repaired TOF has been superseded by non-invasive, often superior imaging with a combination of an echocardiogram and CMR. It remains part of the diagnostic work-up for patients being considered for percutaneous pulmonary valve implantation. This test is valuable in measuring the right ventricular pressure, identifying the level of the obstruction in the RVOT through to the branch pulmonary arteries. Interrogation of the RV outflow tract with a low pressure soft balloon allows sizing of the outflow tract with simultaneous coronary interrogation. Evaluating the coronary arteries and their proximity to the pulmonary conduit is also one of the purposes of this study (Fig. 17).
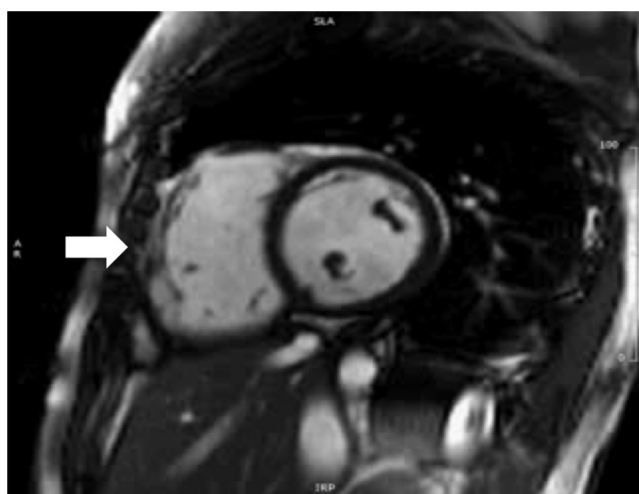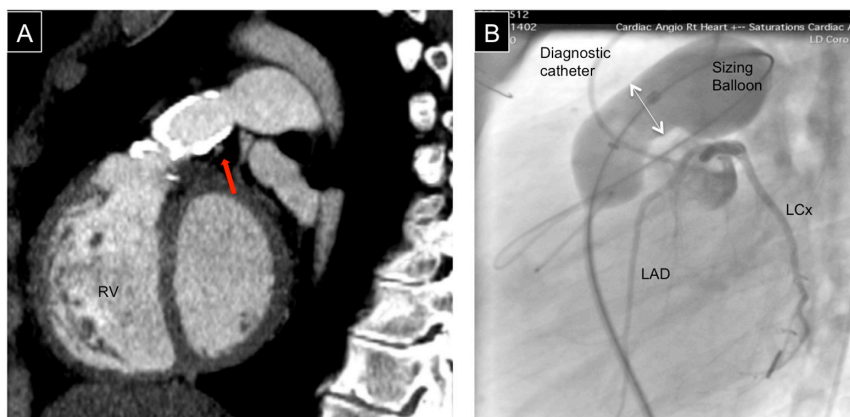
Figure 17

Assessment of suitability for percutaneous pulmonary valve implantation. Contrast cardiac CT (A) showing calcification in an RV–PA conduit (pulmonary homograft) in a patient with previous pulmonary atresia-VSD repair showing heavy calcification and position of the proximal left anterior descending (LAD) coronary artery in relation to the conduit indicated by the red arrow. Cardiac catheter with simultaneous balloon interrogation of the conduit and left coronary angiography (B) allows profiling of the conduit shows that the narrowest segment of the conduit (white arrow) is relatively distant from the LAD. LAD, left anterior descending coronary artery; LCx, left circumflex coronary artery; PA, pulmonary artery; RV, right ventricle.

Conclusion

TOF is one of the commonest congenital heart lesions, with good outcomes from primary surgical repair leading to a growing population of pediatric and adult patients living with this condition. All patients require lifelong follow-up to allow timely identification of the need for further surgery or intervention. Multi-modality imaging is used to consider the need for pulmonary valve replacement, ablation procedures and implantable cardioverter defibrillator implants, although the indications for primary, preventive therapy remain the subjects of debate. The imaging/interventional interface is overlapping in this patient group with fusion imaging already established for electrophysiological and interventional procedures.

References

1 Loffredo CA. Epidemiology of cardiovascular malformations: prevalence and risk factors. *American Journal of Medical Genetics* 2000 **97** 319–325. (https://doi.org/10.1002/1096-8628(200024)97:4<319::AID-AJMG1283>3.0.CO;2-E)

2 Suzuki A, Ho SY, Anderson RH & Deanfield JE. Further morphologic studies on tetralogy of Fallot, with particular emphasis on the prevalence and structure of the membranous flap. *Journal of Thoracic and Cardiovascular Surgery* 1990 **99** 528–535.

3 Ramaswamy P, Lytrivi ID, Thanjan MT, Nguyen T, Srivastava S, Sharma S, Ko HH, Parness IA & Lai WW. Frequency of aberrant subclavian artery, arch laterality, and associated intracardiac anomalies detected by echocardiography. *American Journal of Cardiology* 2008 **101** 677–682. (https://doi.org/10.1016/j.amjcard.2007.10.036)

4 Anderson RH & Weinberg PM. The clinical anatomy of tetralogy of fallot. *Cardiology in the Young* 2005 **15** (Supplement 1) 38–47. (https://doi.org/10.1017/S1047951105001010)

5 Nakata S, Imai Y, Takanashi Y, Kurosawa H, Tezuka K, Nakazawa M, Ando M & Takao A. A new method for the quantitative standardization of cross-sectional areas of the pulmonary arteries in congenital heart diseases with decreased pulmonary blood flow. *Journal of Thoracic and Cardiovascular Surgery* 1984 **88** 610–619.

6 Dabizzi RP, Caprioli G, Aiazzi L, Castelli C, Baldrighi G, Parenzan L & Baldrighi V. Distribution and anomalies of coronary arteries in tetralogy of fallot. *Circulation* 1980 **61** 95–102. (https://doi.org/10.1161/01.CIR.61.1.95)

7 Need LR, Powell AJ, del Nido P & Geva T. Coronary echocardiography in tetralogy of fallot: diagnostic accuracy, resource utilization and surgical implications over 13 years. *Journal of the American College of Cardiology* 2000 **36** 1371–1377. (https://doi.org/10.1016/S0735-1097(00)00862-7)

8 Lev M & Eckner FA. The pathologic anatomy of tetralogy of fallot and its variations. *Diseases of the Chest* 1964 **45** 251–261. (https://doi.org/10.1378/chest.45.3.251)

9 Poon LC, Huggon IC, Zidere V & Allan LD. Tetralogy of Fallot in the fetus in the current era. *Ultrasound in Obstetrics and Gynecology* 2007 **29** 625–627. (https://doi.org/10.1002/uog.3971)

10 Valsangiacomo Buechel ER, Grosse-Wortmann L, Fratz S, Eichhorn J, Sarikouch S, Greil GF, Beerbaum P, Bucciarelli-Ducci C, Bonello B, Sieverding L, *et al*. Indications for cardiovascular magnetic resonance in children with congenital and acquired heart disease: an expert consensus paper of the Imaging Working Group of the AEPC and the Cardiovascular Magnetic Resonance Section of the EACVI. *European Heart Journal: Cardiovascular Imaging* 2015 **16** 281–297. (https://doi.org/10.1093/ehjci/jeu129)

11 Rigsby CK, McKenney SE, Hill KD, Chelliah A, Einstein AJ, Han BK, Robinson JD, Sammet CL, Slesnick TC & Frush DP. Radiation dose management for pediatric cardiac computed tomography: a report from the Image Gently 'Have-A-Heart' campaign. *Pediatric Radiology* 2018 **48** 5–20. (https://doi.org/10.1007/s00247-017-3991-x)

12 Habib Geryes B, Calmon R, Donciu V, Khraiche D, Warin-Fresse K, Bonnet D, Boddaert N & Raimondi F. Low-dose paediatric cardiac and thoracic computed tomography with prospective triggering: is it possible at any heart rate? *Physica Medica* 2018 **49** 99–104. (https://doi.org/10.1016/j.ejmp.2018.05.015)

13 Taussig HB & Blalock A. The tetralogy of Fallot; diagnosis and indications for operation; the surgical treatment of the tetralogy of Fallot. *Surgery* 1947 **21** 145.

14 Sandoval JP, Chaturvedi RR, Benson L, Morgan G, Van Arsdell G, Honjo O, Caldarone C & Lee KJ. Right ventricular outflow tract stenting in tetralogy of fallot infants with risk factors for early primary repair. *Circulation: Cardiovascular Interventions* 2016 **9** e003979. (https://doi.org/10.1161/CIRCINTERVENTIONS.116.003979)

15 Lillehei CW, Cohen M, Warden HE, Read RC, Aust JB, Dewall RA & Varco RL. Direct vision intracardiac surgical correction of the tetralogy of Fallot, pentalogy of Fallot, and pulmonary atresia defects; report of first ten cases. *Annals of Surgery* 1955 **142** 418–442. (https://doi.org/10.1097/00000658-195509000-00010)

16 Chiu SN, Wang JK, Chen HC, Lin MT, Wu ET, Chen CA, Huang SC, Chang CI, Chen YS, Chiu IS, *et al*. Long-term survival and unnatural deaths of patients with repaired tetralogy of Fallot in an Asian cohort. *Circulation: Cardiovascular Quality and Outcomes* 2012 **5** 120–125. (https://doi.org/10.1161/CIRCOUTCOMES.111.963603)

17 Mongeon FP, Gurvitz MZ, Broberg CS, Aboulhosn J, Opotowsky AR, Kay JD, Valente AM, Earing MG, Lui GK, Fernandes SM, *et al*. Aortic root dilatation in adults with surgically repaired tetralogy of fallot: a multicenter cross-sectional study. *Circulation* 2013 **127** 172–179. (https://doi.org/10.1161/CIRCULATIONAHA.112.129585)

18 Khairy P, Dore A, Poirier N, Marcotte F, Ibrahim R, Mongeon FP & Mercier LA. Risk stratification in surgically repaired tetralogy of Fallot. *Expert Review of Cardiovascular Therapy* 2009 **7** 755–762. (https://doi.org/10.1586/erc.09.38)

19 Lang RM, Badano LP, Mor-Avi V, Afilalo J, Armstrong A, Ernande L, Flachskampf FA, Foster E, Goldstein SA, Kuznetsova T, *et al*. Recommendations for cardiac chamber quantification by echocardiography in adults: an update from the American Society of Echocardiography and the European Association of Cardiovascular Imaging. *European Heart Journal: Cardiovascular Imaging* 2015 **16** 233–270. (https://doi.org/10.1093/ehjci/jev014)

20 Koestenberger M, Nagel B, Avian A, Ravekes W, Sorantin E, Cvirn G, Beran E, Halb V & Gamillscheg A. Systolic right ventricular function in children and young adults with pulmonary artery hypertension secondary to congenital heart disease and tetralogy of Fallot: tricuspid annular plane systolic excursion (TAPSE) and magnetic resonance imaging data. *Congenital Heart Disease* 2012 **7** 250–258. (https://doi.org/10.1111/j.1747-0803.2012.00655.x)

21 van der Hulst AE, Roest AA, Delgado V, Holman ER, de Roos A, Blom NA & Bax JJ. Relationship between temporal sequence of right ventricular deformation and right ventricular performance in patients with corrected tetralogy of Fallot. *Heart* 2011 **97** 231–236. (https://doi.org/10.1136/hrt.2010.199919)

22 Srinivasan C, Sachdeva R, Morrow WR, Greenberg SB & Vyas HV. Limitations of standard echocardiographic methods for quantification of right ventricular size and function in children and young adults. *Journal of Ultrasound in Medicine* 2011 **30** 487–493. (https://doi.org/10.7863/jum.2011.30.4.487)

23 Menting ME, van den Bosch AE, McGhie JS, Eindhoven JA, Cuypers JA, Witsenburg M, Geleijnse ML, Helbing WA & Roos-Hesselink JW. Assessment of ventricular function in adults with repaired tetralogy of Fallot using myocardial deformation imaging. *European Heart Journal: Cardiovascular Imaging* 2015 **16** 1347–1357. (https://doi.org/10.1093/ehjci/jev090)

24 Mercer-Rosa L, Parnell A, Forfia PR, Yang W, Goldmuntz E & Kawut SM. Tricuspid annular plane systolic excursion in the assessment of right ventricular function in children and adolescents after repair of tetralogy of Fallot. *Journal of the American Society of Echocardiography* 2013 **26** 1322–1329. (https://doi.org/10.1016/j.echo.2013.06.022)

25 Kutty S, Zhou J, Gauvreau K, Trincado C, Powell AJ & Geva T. Regional dysfunction of the right ventricular outflow tract reduces the accuracy of Doppler tissue imaging assessment of global right ventricular systolic function in patients with repaired tetralogy of Fallot. *Journal of the American Society of Echocardiography* 2011 **24** 637–643. (https://doi.org/10.1016/j.echo.2011.01.020)

26 Baumgartner H, Bonhoeffer P, De Groot NM, de Haan F, Deanfield JE, Galie N, Gatzoulis MA, Gohlke-Baerwolf C, Kaemmerer H, Kilner P, *et al*. ESC Guidelines for the management of grown-up congenital heart disease (new version 2010). *European Heart Journal* 2010 **31** 2915–2957. (https://doi.org/10.1093/eurheartj/ehq249)

27 Stout KK, Daniels CJ, Aboulhosn JA, Bozkurt B, Broberg CS, Colman JM, Crumb SR, Dearani JA, Fuller S, Gurvitz M, *et al*. 2018 AHA/ACC guideline for the management of adults with congenital heart disease: executive summary: a report of the American College of Cardiology/American Heart Association Task Force on Clinical Practice Guidelines. *Journal of the American College of Cardiology* 2018 [epub]. (https://doi.org/10.1016/j.jacc.2018.08.1028)

28 Therrien J, Provost Y, Merchant N, Williams W, Colman J & Webb G. Optimal timing for pulmonary valve replacement in adults after tetralogy of Fallot repair. *American Journal of Cardiology* 2005 **95** 779–782. (https://doi.org/10.1016/j.amjcard.2004.11.037)

29 Ammash NM, Dearani JA, Burkhart HM & Connolly HM. Pulmonary regurgitation after tetralogy of Fallot repair: clinical features, sequelae, and timing of pulmonary valve replacement. *Congenital Heart Disease* 2007 **2** 386–403. (https://doi.org/10.1111/j.1747-0803.2007.00131.x)

30 Geva T. Indications and timing of pulmonary valve replacement after tetralogy of Fallot repair. *Seminars in Thoracic and Cardiovascular Surgery: Pediatric Cardiac Surgery Annual* 2006 **9** 11–22. (https://doi.org/10.1053/j.pcsu.2006.02.009)

31 Frigiola A, Redington AN, Cullen S & Vogel M. Pulmonary regurgitation is an important determinant of right ventricular contractile dysfunction in patients with surgically repaired tetralogy of Fallot. *Circulation* 2004 **110** (11 Supplement 1) II153–II157. (https://doi.org/10.1161/01.CIR.0000138397.60956.c2)

32 Ferraz Cavalcanti PE, Sa MP, Santos CA, Esmeraldo IM, de Escobar RR, de Menezes AM, de Azevedo OM Jr, de Vasconcelos Silva FP, Lins RF, *et al*. Pulmonary valve replacement after operative repair of tetralogy of Fallot: meta-analysis and meta-regression of 3,118 patients from 48 studies. *Journal of the American College of Cardiology* 2013 **62** 2227–2243. (https://doi.org/10.1016/j.jacc.2013.04.107)

33 Bokma JP, Geva T, Sleeper LA, Babu Narayan SV, Wald R, Hickey K, Jansen K, Wassall R, Lu M, Gatzoulis MA, *et al*. A propensity score-adjusted analysis of clinical outcomes after pulmonary valve replacement in tetralogy of Fallot. *Heart* 2018 **104** 738–744. (https://doi.org/10.1136/heartjnl-2017-312048)

34 Goreczny S, Moszura T, Dryzek P, Lukaszewski M, Krawczuk A, Moll J & Morgan GJ. Three-dimensional image fusion guidance of percutaneous pulmonary valve implantation to reduce radiation exposure and contrast dose: a comparison with traditional two-dimensional and three-dimensional rotational angiographic guidance. *Netherlands Heart Journal* 2017 **25** 91–99. (https://doi.org/10.1007/s12471-016-0941-4)